$CF_3CH_3 \rightarrow HF + CF_2CH_2$: A Non-RRKM Reaction?†

John R. Barker,*,⊥,‡ Philip J. Stimac,⊥ Keith D. King,§ and David M. Leitner||

Department of Atmospheric, Oceanic, and Space Sciences, University of Michigan, Ann Arbor, Michigan 48109-2143, Department of Chemistry, University of Michigan, Ann Arbor, Michigan 48109-1055, School of Chemical Engineering, University of Adelaide, Adelaide 5005 SA, Australia, and Department of Chemistry, University of Nevada, Reno, Nevada 89557

Received: August 11, 2005; In Final Form: September 30, 2005

The experimental shock tube data recently reported by Kiefer et al. [*J. Phys. Chem. A* **2004**, *108*, 2443−2450] for the title reaction at temperatures between 1600 and 2400 K have been compared to master equation simulations using three models: (a) standard RRKM theory, (b) RRKM theory modified by local random matrix theory, which introduces dynamical corrections arising from slow intramolecular vibrational energy randomization, and (c) an ad hoc empirical non-RRKM model. Only the third model provides a good fit of the Kiefer et al. unimolecular reaction rate data. In separate simulations, all three models accurately reproduce the experimental 300 K chemical activation data of Marcoux and Setser [*J. Phys. Chem.* **1978**, *82*, 97−108] when the energy transfer parameters are freely varied to fit the data. When experimental energy transfer parameters for a geometrical isomer (1,1,2-trifluoroethane) are used, the standard RRKM model fits the chemical activation data better than the other models, but if energy transfer in the 1,1,1-trifluoroethane is significantly reduced in comparison to the 1,1,2 isomer, then the empirical ad hoc non-RRKM model also gives a good fit. While the ad hoc empirical non-RRKM model can be made to fit the data, it is not based on theory, and we argue that it is physically unrealistic. We also show that the master equation simulations can mimic the Kiefer et al. vibrational relaxation data, which was the first shock tube observation of double-exponential relaxation. We conclude that, until more data on the trifluoroethanes become available, the current evidence is insufficient to decide with confidence whether non-RRKM effects are important in this reaction, or whether the Kiefer et al. data can be explained in some other way.

I. Introduction

Recently, Kiefer et al.[1] (KKSST) reported schlieren shock tube experiments in which they measured vibrational relaxation, incubation, and unimolecular rate constants for the title reaction as functions of temperature and pressure (see Figure 1). They analyzed their data set by attempting to fit it using the conventional modified strong collision version of RRKM theory.[2−6] They found that, while the RRKM model predicts that the rate constants should continue to increase with pressure, their data at the two highest pressures (350 and 550 Torr) fall essentially on the same line as their 100 Torr data. KKSST also noted that their vibrational relaxation data could be modeled by a double exponential decay. To explain these observations, they invoked a breakdown of RRKM theory due to slow intramolecular vibrational energy redistribution (IVR), probably associated with the internal rotor in 1,1,1-trifluoroethane (TFE). (See Appendix III for a critique of their model.)

Breakdowns of RRKM theory are relatively rare for thermal activation reactions with high barriers.[3,5] RRKM theory as it stands today is the culmination of about 80 years of development, in particular by O. K. Rice, H. C. Ramsperger, L. S. Kassel, and R. A. Marcus, and later by many other workers (see the brief historical introduction in Forst's recent book[3]). The theory has been extremely successful. It is the current standard against which virtually all unimolecular (and recombination) reaction rate data are assessed, and it provides a basis for predicting unimolecular (and recombination) reaction rate

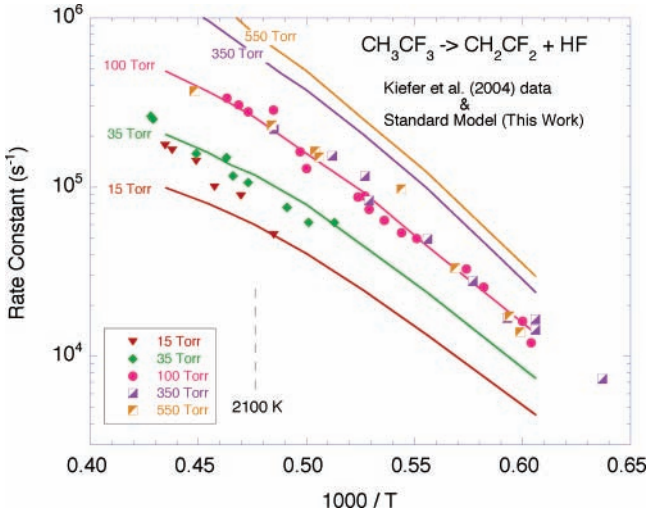

Figure 1. Unimolecular rate constants from the KKSST experiments (points) and calculated using the standard (fast-IVR) model (lines). To obtain the lines, unimolecular rate constants were calculated for a number of temperatures and the data points connected by straight line segments. Fluctuations in the lines are caused by stochastic uncertainties[12] due to the finite number of stochastic trials carried out to calculate each rate constant datum.

† Part of the special issue "Jürgen Troe Festschrift".

* Corresponding author: jrbarker@umich.edu.
⊥ Department of Atmospheric, Oceanic, and Space Sciences, University of Michigan.
‡ Department of Chemistry, University of Michigan.
§ University of Adelaide.
|| University of Nevada.

10.1021/jp054510x CCC: $33.50
Published on Web 12/15/2005

TABLE 1: Arrhenius Parameters for Thermal HF Elimination from TFE

A_∞ (s^{-1})	E_∞ (kcal mol^{-1})	temp. range (K)	pressure range (bar)	ref
1.4×10^{12}	61.40	843−923	1.01	Sianesi et al. (1968)
6.3×10^{13}	73.73	1590−1680	1.07−1.20 (in Ar)	Cadman et al. (1971)
1.0×10^{14}	68.76	1080−1310	3.20−4.53 (in Ar)	Tschuikow-Roux and Quiring (1971)
8.0×10^{14}	69.5			Tsang[a] (1973)
4.0×10^{14}	72.53	1000−1800		Rodgers and Ford[b] (1973)
7.0×10^{14}	74.12	1050−1200	2.53 (in Ar)	Tsang and Lifshitz[c] (1998)
3.5×10^{14}	71 ± 3			Martell, Beaton, and Holmes[d] (2002)
1.58×10^{15}	75.033	1600−2400	15−550 Torr (in Kr)	KKSST[e] (2004)

[a] Reanalysis of the data of Cadman et al. [b] Reanalysis of the data of Sianesi et al., Cadman et al., and Tschuikow-Roux and Quiring. [c] RRKM extrapolation to the high-pressure limit. [d] Based on $k_\infty = 1.4 \pm 1.0 \times 10^{-5}$ s^{-1} at 800 K and average $E_\infty = 71 \pm 3$ kcal mol^{-1} from the shock-tube results of Tsang and Lifshitz, Tschuikow-Roux and Quiring, and Sianesi et al. [e] Obtained from an Arrhenius plot of k_∞ calculated from G3/TST.

constants from basic principles. Since there is so much reliance on the accuracy of RRKM theory, it is important to determine whether the theory has failed for the title reaction, or whether some other explanation of the KKSST data must be sought.

What is the reason for the discrepancy between the KKSST data set and RRKM theory? In the present paper, we address this question by determining to what extent the KKSST data are consistent with a full RRKM/master equation treatment,[12] with the IVR theory described by Leitner and Wolynes,[7−11] with a strictly empirical non-RRKM adjustment of $k(E)$, and with other extant data on trifluroroethane(s). Our approach is to simulate the KKSST shock experiments with the MultiWell master equation code.[12,13] We also simulate some of the many experiments in the literature on TFE thermal activation[14−17] and chemical activation.[18]

As discussed below, we find that the KKSST data at the two highest pressures are not consistent with either RRKM theory ("standard" model) or the theoretical modification to include slow IVR ("slow-IVR" model).[7−11] We show that it is possible to fit the KKSST data by empirically modifying $k(E)$ and that the same model ("truncated" model) will also fit the chemical activation data of Marcoux and Setser[19] when no constraints are placed on empirical parameters for energy transfer. However, when the energy transfer parameters are estimated from a proxy (the 1,1,2-TFE isomer), the chemical activation data are more consistent with standard RRKM theory than with the empirical "truncated" model that describes the KKSST data. While the "truncated" model fits the KKSST data, it is not based on theory, and we argue that it is physically unrealistic. Additionally, we show that a conventional master equation that obeys RRKM theory can produce vibrational relaxation with two (or more) time constants. In the end, however, it is still not possible to determine whether there has been a breakdown of RRKM theory, or whether the KKSST data can be explained in some other way. Classical trajectory calculations are being performed in our lab to provide further information about IVR in this system.[20]

II. Background

A. Thermal and Chemical Activation Experiments. A number of thermal studies of TFE kinetics were carried out prior to the work of KKSST, but all were at lower temperatures and at relatively high pressures, where falloff is less important. Thermal decomposition studies were conducted by Sianesi et al.,[21] who used a heated flow tube reactor, and by Cadman et al.,[15] Tschuikow-Roux and Quiring,[14] and Tsang and Lifshitz,[16] all of whom used shock tubes. The Arrhenius parameters from all four studies are shown in Table 1. The parameters obtained by Sianesi et al. are unusually low in comparison with the other studies. The estimated temperatures in the shock tube study carried out by Cadman et al. have been questioned by others and considered to be too low by several hundred degrees. Tsang[22] reanalyzed the data of Cadman et al. and recommended Arrhenius parameters as shown in Table 1. The original kinetic data of all the above four studies were analyzed by Rodgers and Ford,[23] and their recommended Arrhenius parameters are also shown in Table 1.

Martell, Beaton, and Holmes[24] (MBH) examined the four studies mentioned above in terms of the Arrhenius parameters and by comparing the high-pressure rate constant, k_∞ at 800 K. They adopted $k_\infty = (1.4 \pm 1.0) \times 10^{-5}$ s^{-1} at 800 K (average of the shock tube results of Tsang and Lifshitz,[16] Tschuikow-Roux and Quiring[14] and Sianesi et al.[21]) and combined it with an average activation energy of 71 ± 3 kcal mol^{-1} from the shock tube results to yield $A_\infty = 3.5 \times 10^{14}$ s^{-1}.

HF elimination from chemically activated TFE has been studied by Pettijohn, Mutch, and Root[25] in a hot atom experiment involving ^{18}F atoms. They concluded that the reaction system does not agree with RRKM theory, but their conclusion is weakened because of the poorly defined energy distributions produced with this technique. Neely and Carmichael[26] used $CH_3 + CF_3$ recombination as the preparation method, as did Setser and co-workers[19,27] who used the same preparation method but took appropriate steps to avoid the complications caused by subsequent removal of CH_2CF_2 (product from HF elimination) by reaction with CF_3. Indeed, Ferguson et al.[28] consider the Marcoux and Setser data set[19] to be the best available from chemical activation experiments. The Marcoux and Setser data set is modeled in the calculations described below.

In the chemical activation experiments, excited TFE was produced at 300 K with ∼101 kcal mol^{-1} of vibrational excitation[24,28] in the exothermic recombination reaction of CF_3 with CH_3, followed by HF elimination in competition with collisional stabilization

$$CF_3 + CH_3 \rightarrow CF_3CH_3^* \quad (1)$$

$$CF_3CH_3^* \rightarrow CF_2CH_2 + HF \quad \text{Decomposition (D)} \quad (2)$$

$$CF_3CH_3^* + M \rightarrow CF_3CH_3 + M \quad \text{Stabilization (S)} \quad (3)$$

Experiments were conducted at 300 K with 17 bath gases and at 195 K with 5 bath gases. The high-pressure chemical activation rate constant can be expressed as $k_a = \omega D/S$ or $k_a' = PD/S$, where ω is the collision frequency, P is the pressure, and the D/S ratio is the fraction of excited TFE that decomposes to that which is stabilized in collisions. At sufficiently high pressures, k_a^∞ is independent of pressure. By estimating the Lennard-Jones collision frequency and carrying out a theoretical analysis, Marcoux and Setser[19] found $k_a^\infty = (3.2 \pm 0.3) \times 10^8$ s^{-1}.

B. Vibrational Relaxation Experiments. KKSST measurements of vibrational relaxation in the TFE system are the first to have observed dual vibrational relaxation processes using a shock tube. Kiefer and co-workers previously measured "nonlinear" relaxation in a number of molecules.[29] Very recently, the Kiefer group reported dual vibrational relaxation times and successful RRKM modeling of the ethane decomposition rate constant.[30] They apparently did not attempt to model the vibrational relaxation.

In general, one might always expect to observe multiple time scales for vibrational relaxation, because each internal mode would be expected to relax at its own characteristic rate. However, only rate-limiting steps are observed experimentally, and in most systems, only a single time constant is observed. This time constant is for the slow transfer of translational energy to the lowest vibrational mode of the molecule; subsequent transfer of energy to other modes is much faster (not rate-limiting) and is not observed. For systems that display dual relaxation time constants, the faster process is associated with relaxation of energy in the lowest-frequency mode, and the slower process results from a bottleneck in transferring the energy to the molecule's higher-frequency vibrational modes.[31−33]

If sufficient information is available, vibrational relaxation can be modeled accurately using a state-to-state kinetics model.[31,34] In principle, SSH theory[35,36] or much more accurate infinite-order sudden approximation theories[37,38] can calculate the rate constants, but ab initio approaches are very expensive for molecules with more than a few vibrational modes.

As discussed below, an empirical master equation approach is used in the present work simply to confirm that the observation of multiple time scales of energy transfer low on the energy ladder does not necessarily imply a breakdown of RRKM theory at the much higher vibrational energies needed for reaction.

III. Computational Models

A. Previous Models. An important test of the models is that they should simultaneously simulate both thermal and chemical activation experimental data. However, a major drawback is that because of the large differences in temperature between shock tube and chemical activation experiments the temperature dependence of the energy transfer is a significant unknown factor.

KKSST used Pople's G3 method[39] to calculate the properties of the TFE molecule and transition state, which were then used in RRKM calculations. The CH_3 torsion was treated as a harmonic vibration, because with a calculated barrier to internal rotation of 1137 cm^{-1}, hindered rotor calculations were approximately the same as those for a vibration, especially at the high temperatures of the shock tube experiments. Their calculated rate constants are in excellent agreement with previous shock tube data obtained at higher pressures and lower temperatures.

Transition state theory (TST) models used to interpret chemical activation data on TFE were used by Chang, Craig, and Setser,[27] Marcoux and Setser,[19] MBH,[24] and Ferguson et al.[28] Chang, Craig, and Setser used traditional four-centered TST models for HX elimination from haloalkanes. MBH tested a range of ab initio and density functional theory (DFT) calculations and found that all calculations yielded quite similar results for molecular vibrational frequencies and moments of inertia, in agreement with experimental data.

B. Master Equation. Rate constants for dissociation depend on both vibrational energy and angular momentum, as does collisional energy transfer. For tight transition states, as in the title reaction, angular momentum effects are small. In the present work, centrifugal corrections are applied by using the pseudodiatomic approximation[2] and by assuming that the energy in the "K-rotor" (nonconserved rotational degree of freedom) mixes freely with energy that resides in the other active degrees of freedom and is limited only by the total active energy. The MultiWell software package[12,13,40] was used for all of the calculations.

According to RRKM theory,[2,4,6] the energy-dependent specific unimolecular rate constant $k(E)$ is given by

$$k(E) = \left[\frac{m^{\ddagger}}{m}\frac{\sigma_{\mathrm{ext}}}{\sigma_{\mathrm{ext}}^{\ddagger}}\right]\frac{g_{\mathrm{e}}^{\ddagger}}{g_{\mathrm{e}}}\frac{1}{h}\frac{G^{\ddagger}(E-E_0)}{\rho(E)} \qquad (4)$$

where $m^{\ddagger}$ and m are the number of optical isomers, $\sigma_{\mathrm{ext}}^{\ddagger}$ and σ_{ext} are the external rotation symmetry numbers, and $g_{\mathrm{e}}^{\ddagger}$ and g_{e} are the electronic state degeneracies of the transition state and reactant, respectively; h is Planck's constant, $G^{\ddagger}(E - E_0)$ is the sum of states of the transition state, E_0 is the reaction threshold energy, and $\rho(E)$ is the density of states of the reactant molecule. The internal energy E is measured relative to the zero-point energy of the reactant molecule, and the reaction threshold energy (critical energy) is the difference between the zero-point energies of reactant and transition state. Equation 1 is written with the assumption that the rotational *external* symmetry numbers, electronic degeneracies, and numbers of optical isomers were *not* used in calculating the sums and densities of states, but the *internal* rotor symmetry numbers are used explicitly and hence do not appear in eq 3. Note that the quantity set off in square brackets is the reaction path degeneracy, which is equal to 3 for reaction 2. See Appendix I for a discussion of how the reaction path degeneracy was determined for this system.

Specific rate constants for reaction 2 are calculated using RRKM theory,[2,4−6] which requires calculation of the densities of internal states for the potential well and the sum of states for transition state for reaction 2. Normal-mode vibrational frequencies and moments of inertia for TFE and the transition state were taken from KKSST, with the following small changes: (a) The TFE frequency at 249 cm^{-1} is treated (approximately[41]) as a threefold hindered internal rotation with barrier height equal to 1137 cm^{-1}; (b) the imaginary frequency (2027 cm^{-1}) of the transition state for reaction 2 is from Martell et al.[24] All of the sums and densities of states are calculated (program DenSum[13]) by "exact counts", using the Beyer−Swinehart algorithm[42] as adapted by Stein and Rabinovitch.[43] Tests showed that an energy grain size of $\leq$10 cm^{-1} gives accurate results for steady-state unimolecular rate constants, but a smaller grain size ($\leq$3 cm^{-1}) is necessary for converged calculations of the vibrational energy relaxation following the shock.

In recombination reactions, such as reaction 1, the two reactants come together to form a highly excited adduct, which can redissociate, be collisionally deactivated, and react via reaction 2. The chemical activation energy distribution[2−6] (implemented in MultiWell[12]) describes the nascent energy distribution in the highly excited adduct. In the present work, the rate constant for C−C bond fission (reaction (−1)) was approximated using the inverse Laplace transform (ILT) method of Forst.[2,3] The Arrhenius parameters for reaction (−1) (needed for the ILT method) were obtained from the equilibrium constant and the measured recombination rate constant.[18]

In the present work, collision frequencies are calculated by using Lennard-Jones parameters[1] for krypton (σ_{Kr} = 4.959,

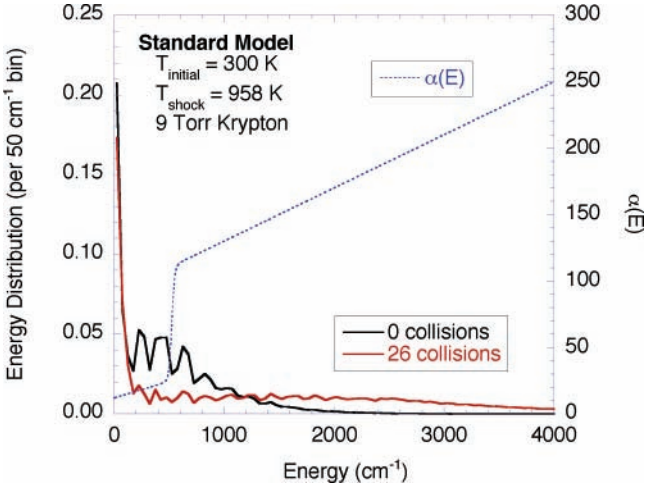

Figure 2. The functional form of α(*E*), as defined by eqs 6a and b, is shown as a dotted line. The transition between two distinct energy regimes is at 525 cm^{-1} (parameter b_1 in eq 6b), and the width of the transition is 25 cm^{-1} (parameter b_2 in eq 6b). The other parameters of eq 6 used in the MultiWell simulations are as follows: $c_{11} = 12$ cm^{-1}, $c_{12} = 0.025$, $c_{21} = 90$ cm^{-1}, and $c_{22} = 0.04$. The two traces represent the fraction of molecules per 50 cm^{-1} energy bin at the beginning of the simulation (black trace) and after 26 collisions (red trace).

$\epsilon_{Kr}/K = 387$ K) and TFE ($\sigma_{TFE} = 3.61$ Å, $\epsilon_{TFE}/K = 190$ K) with the usual combining rules and formulas.[12] The conventional exponential-down model for the collision step size distribution is assumed

$$P(E, E') = \frac{1}{N(E')} \exp\left[\frac{-(E' - E)}{\alpha(E')}\right] \quad \text{for } (E' - E) \geq 0 \quad (5)$$

where $P(E, E')$ is the probability density for energy transfer from vibrational energy E' to energy E in a deactivation step, $N(E')$ is a normalization factor, and the energy transfer parameter α(E') is a function of internal energy and temperature. The temperature dependence of α(E') is not known. As discussed below, this lack of knowledge is a significant impediment to determining whether the high-temperature shock tube data are consistent with the low-temperature chemical activation data.

The energy dependence of α(E') is critically important in simulating vibrational relaxation following a shock.[44,45] To simulate a dual relaxation somewhat like that measured by KKSST, it is necessary to introduce a bottleneck to energy transfer at low vibrational energies. In the present work, this is accomplished with the following function for α(E'):

$$\alpha(E') = [1 - S(E')]\{c_{11} + c_{12}E'\} + S(E')\{c_{21} + c_{22}E'\} \quad (6a)$$

where $S(E')$ is a switching function

$$S(E') = \frac{1}{2}\left[1 - \tanh\left(\frac{E' - b_1}{b_2}\right)\right] \quad (6b)$$

In these expressions, the coefficients c_{ij} and b_k are empirical parameters. The central energy at which the switch takes place is defined by parameter b_1, and the energy range over which it takes place is controlled with parameter b_2. The net effect of these expressions is to switch between two simple linear functions of energy, as shown in Figure 2. Recent "direct" experiments on collisional vibrational energy transfer are consistent with a linear energy dependence at vibrational energies greater than ~5000 cm^{-1}.[46]

C. Vibrational Energy Flow and Non-RRKM Kinetics. An inherent assumption embodied in RRKM theory is that energy is rapidly redistributed among all vibrational modes of the molecule, at least as fast as the barrier-crossing frequency. For this assumption to hold, the population of molecules that are in an activated complex and poised to react must rapidly reequilibrate following reaction. Reequilibration can occur by IVR or through collisions. These processes must thus occur on a time scale faster than the barrier crossing frequency. If the barrier energy is high, energy flow may indeed be sufficiently rapid. If the barrier energy is not so high, such as a barrier to conformational change, energy flow may be limited or sufficiently slow to influence the reaction rate.[7,9,10,47−52]

If k_{IVR} is the IVR rate, including effects of collisions, then the microcanonical rate, $k(E)$, is[7,9,49]

$$k(E) = \kappa(E)k_{RRKM}(E) \quad (7a)$$

$$\kappa(E) = \frac{k_{IVR}(E)}{k_{IVR}(E) + \nu_R(E)} \quad (7b)$$

$$k_{IVR}(E) = k^q_{IVR}(E) + k^c_{IVR}[M] \quad (7c)$$

where ν_R is the barrier-crossing frequency and $\kappa(E)$ is the IVR transmission coefficient. The rate, k_{IVR}, has contributions from both collision-free IVR, k^q_{IVR} (calculated quantum mechanically below), and collision-induced[49] IVR, $k^c_{IVR}[M]$, where k^c_{IVR} is an effective collision rate constant and [M] is the concentration of collider gas.

To compute dynamical corrections to RRKM theory, we must first compute the extent and rate of IVR. To locate the IVR threshold, beyond which vibrational energy flows freely over the energy shell, we turn to local random matrix theory (LRMT),[53] which has been developed to describe quantum mechanical energy flow and localization in many nonlinear oscillator systems,[53−55] such as the vibrations of a modest-sized molecule. Local random matrix theory reveals that the IVR threshold does not directly depend on the total density of states of the molecule, but on a local density of resonantly coupled states.[53,54]

The IVR transition lies at the energy where the local density of states coupled anharmonically to states on the energy shell times the strength of the anharmonic coupling is of the order 1. More specifically, IVR is unrestricted when[53]

$$T(E) \equiv \sqrt{\frac{2\pi}{3}} \sum_Q \langle |V_Q| \rangle \rho_Q \geq 1 \quad (8)$$

where Q is the distance in vibrational quantum number space between two states coupled by the matrix element V_Q. We obtain the local density of states, ρ_Q, coupled by all orders of anharmonicity to any given state on the energy shell by direct count using the vibrational frequencies.

We obtain the anharmonic matrix elements following the scaling relations determined by Gruebele et al.[55−58] We estimate the anharmonic matrix elements, V_{ij}, coupling states $|i\rangle$ and $|j\rangle$ using the formulas[55−58]

$$V_{ii'} = \prod_\alpha R_\alpha^{n_\alpha} \quad (9a)$$

$$R_\alpha \approx \frac{a^{1/Q}}{b}(\omega_\alpha \bar{\nu}_\alpha)^{1/2} \quad (9b)$$

$$Q = \sum_\alpha n_\alpha \quad (9c)$$

where n_α is the occupation number difference between two normal modes, α' and α, for basis states $n_\alpha = \sum|\nu_{\alpha'} - \nu_\alpha|$; and a and b are constants. If V_{ij} is expressed in reciprocal centimeters, then $a \approx 3000$ and $b \approx 200-300$. We use $a = 3050$ and $b = 270$ in our calculations. We also compute IVR rates, $k^q_{IVR}(E)$, at energies above the threshold. At energies well above the threshold energy, we can estimate this rate, $k^{q,\infty}_{IVR}(E)$, as

$$k^{q,\infty}_{IVR}(E) = \frac{2\pi}{\hbar}\sum_Q |V_Q|^2 \rho_Q(E) \qquad (10)$$

Just above the IVR threshold, the IVR rate must go smoothly from 0, at the threshold, to the value given by eq 6. We model this behavior with the form[53,55]

$$k^q_{IVR} = k^{q,\infty}_{IVR}\sqrt{1 - T(E)^{-1}} \quad T(E) \geq 1 \qquad (11)$$

where $T(E)$, defined by eq 8, must be ≥ 1 for energy to flow freely over the energy shell.

LRMT has been applied to predict the ergodicity threshold, the dilution factor below the threshold, and energy flow rates above it for dozens of modest-sized organic molecules, generally comparing well with experimental results.[9,11,56] It has been applied extensively to conformational isomerization reactions, explaining why rates are often observed to be orders of magnitude slower than predicted by RRKM theory.[7,9,10,47] For example, calculations based on LRMT correctly describe the variation of the rate of cyclohexane ring inversion with pressure, which RRKM theory does not, and provide a good estimate for the rate.[7] The rates of *trans*-stilbene photoisomerization in molecular beam and in bulb experiments, which again RRKM theory fails to predict, have also been well-described by LRMT.[9,10]

The LRMT was developed to predict the ergodicity threshold and k^q_{IVR} at low to moderate energies above the threshold, where it has had considerable success. At higher energies, it predicts IVR rates that increase steadily with energy, resulting in the expected approach to unity by the IVR transmission coefficient (eq 7b). At very high energies, the LRMT predicts IVR rates that are too fast to be physically reasonable. Energy flow cannot be arbitrarily fast, since the vibrational time scale of the oscillators, roughly half a vibrational period, limits the time for energy to travel in the molecule. Thus, an upper limit of $2\langle\nu\rangle$ is placed on $k^q_{IVR}(E)$ in the present calculations, where $\langle\nu\rangle$ is the average vibrational frequency.

IV. Results

A. Vibrational Relaxation. Input parameters for the MultiWell calculations are described in Appendix II. For the MultiWell double arrays,[12] 1500 array elements were used for the low-energy regime, 500 array elements were used for the high-energy regime, and the energy ceiling was set at 50 000 cm^{-1}.

Parameters c_{21} and c_{22} in eq 6a were obtained by simulating the KKSST rate constant data at 100 Torr. This pressure was chosen because it is the central pressure in their data set; we note that Kiefer has stated (private communication) that the experimental setup was optimal for this pressure. The remaining parameters in eq 6 were chosen to reproduce the KKSST vibrational relaxation times for 9 Torr and 958 K (Figure 6 in KKSST). The functional form of eq 6 and the energy transfer function $\alpha(E)$ are given in Figure 2. Also shown in Figure 2 are the 300 K thermal vibrational energy distribution at the beginning of the simulation and the energy distribution after 26 collisions have taken place.

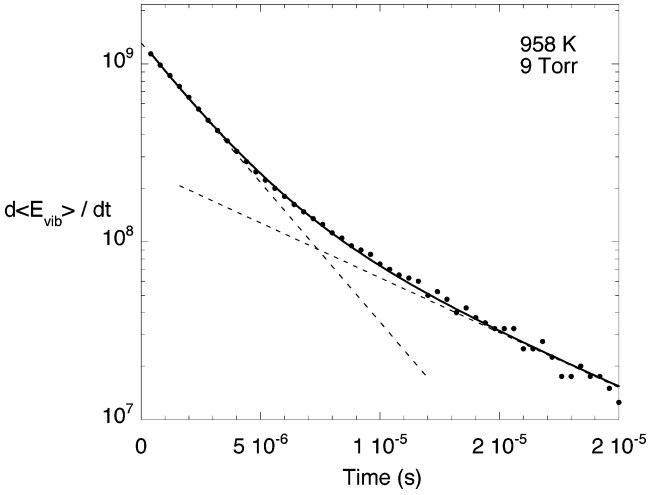

Figure 3. Vibrational relaxation for 958 K and 9 Torr of krypton. The points are obtained from MultiWell, and the solid line is a nonlinear least-squares fit to the data using eq 12. The dashed lines emphasize the dual relaxation times.

TABLE 2: Vibrational Relaxation Times as a Function of Temperature for $P_{Kr} = 9$ Torr

temperature (K)	τ_1 (ns atm)	τ_2 (ns atm)
958	26.9	86.2
1200	30.7	88.4
1400	30.4	91.1
1600	38.8	109.6
1800	37.0	118.4
2000	34.8	140.9

In schlieren shock tube measurements, the signal is proportional to the axial density gradient, which is in turn proportional to the rate of energy transfer.[59,60] In the MultiWell simulations, the average vibrational energy $\langle E_{vib}(t)\rangle$ was calculated as a function of time, and the rate of energy transfer was obtained by taking the numerical time derivative of the average vibrational energy: $d\langle E_{vib}(t)\rangle/dt$. An example simulation is shown in Figure 3.

Much as in the KKSST experiments, the rate of energy transfer in Figure 3 exhibits a dual relaxation. At higher temperatures, the simulated rate of energy transfer often exhibits an initial transient. Following the initial transient, $d\langle E_{vib}(t)\rangle/dt$ is accurately described by a sum of two exponentials

$$\frac{d}{dt}\langle E_{vib}(t)\rangle = -a_1 \exp(-a_2 t) - a_3 \exp(-a_4 t) \qquad (12)$$

where t is time, and parameters a_i ($i = 1, ..., 4$) are obtained by nonlinear least-squares analysis. Vibrational relaxation times (the inverse of the a_2 and a_4 parameters) were obtained by nonlinear least-squares analysis for the time period following the initial transient. Long simulations (4×10^6 stochastic trials) are necessary to reduce the statistical scatter in the time derivative so that reliable vibrational relaxation times can be determined. The relative errors in the fit parameters a_2 and a_4 are generally less than ~5%.

Vibrational relaxation times calculated for a pressure of 9 Torr and select temperatures between 958 and 2000 K are given in Table 2. Overall, the calculated vibrational relaxation times are in good agreement with those measured by KKSST. Despite the small quantitative differences, it is clear that dual vibrational

relaxation times can be obtained for TFE if a suitable energy transfer function is used. In the present empirical approach, the energy transfer parameters are not unique and do not have specific physical interpretations.

It is worth noting that the reaction incubation times resulting from this energy transfer model agree within a factor of ~2 with the experimental data in Figure 9 of KKSST. The experimental incubation time data are reported in "laboratory time", because they were deemed too uncertain for reliable transformation to "molecule time" (J. H. Kiefer, private communication).

B. RRKM/Master Equation Models. *Fast IVR and the KKSST Data Set*. Unimolecular rate constants were obtained from the negative of the slope of the last 20% of plots of $\ln[TFE]/[TFE]_0$ vs time or from the instantaneous average rates reported by MultiWell. Long-time simulations were run to obtain accurate estimates of the steady-state rates. Steady state is reached after about 15−20% of the TFE has reacted; at the end of a simulation, about 10% of the initial TFE still remains. The pressure-dependent rate constants determined from the simulations using the "standard" model with fast IVR are shown in Figure 1.

It is important to carefully examine the experimental data obtained by KKSST, and it is useful to do so in comparison with the standard model, which gives results that are very similar to the simple modified strong-collider RRKM model reported by KKSST. The data at 35 and 100 Torr are in very good agreement with the simulations (which were fitted to the 100 Torr data set). The data sets at 15, 350, and 550 Torr are all in disagreement. At 15 Torr, the data show significantly stronger temperature dependence than the standard model, and the centroid of the data set is at a significantly higher rate constant than the standard model. This strong temperature dependence is also at odds with the data obtained at the other pressures. These systematic discrepancies may be due to the possible susceptibility of this lowest-pressure data set to unidentified systematic experimental errors.[1] The data sets at 350 and 550 Torr essentially fall on top of the data at 100 Torr, while the standard model predicts that both should have significantly larger rate constants. This was one of the major points raised by KKSST and ascribed to the effect of slow IVR. KKSST did not provide objective error estimates that would enable an assessment of the significance of these discrepancies, but state that the scatter of the data provides the best estimate of experimental errors.

Whether or not steady state is achieved in the KKSST experiments is an important issue when considering the accuracy of the KKSST data set. At high pressure, steady state is reached very quickly, but at low pressure, long times (much longer than those studied in the KKSST experiments) are needed to achieve steady state. Since the KKSST data set is unusual at high pressure, we compared the 550 Torr rate constants calculated using data between 2 and 6 μs (roughly the experimental time window accessible by KKSST in their experiments) to those calculated using data for much longer times. We found that the rate constants changed by less than 10%, indicating the KKSST rate data at high pressure were at steady state.

Slow IVR. Using the LRMT criterion for quantum energy flow, eq 8, we find the IVR threshold for TFE to lie around 3500 cm^{-1}, nearly 60 kcal mol^{-1} *below* the reaction critical energy (Figure 4). Above the IVR threshold, we compute the IVR rate with eqs 9 and 10. With the exception of values close to the transition energy, the IVR rate above the threshold is

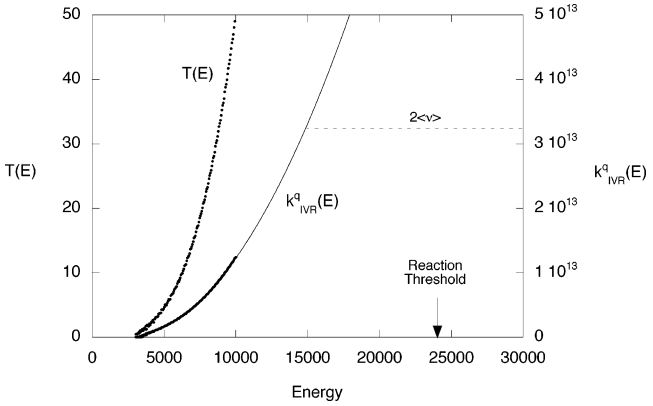

Figure 4. The computed transition parameter, $T(E)$, and rate of vibrational energy flow in the absence of collisions, $k^q_{IVR}(E)$ in units of reciprocal seconds. The IVR threshold energy corresponds to $T(E) = 1$; $k^q_{IVR}(E)$ is finite when $T(E) > 1$. Both quantities are calculated to an energy of 10 000 cm^{-1} (points) and extrapolated (thin solid line) to higher energies. The physical upper limit to $k^q_{IVR}(E)$ is $\sim 2\langle\nu\rangle = 3.2 \times 10^{13}$ s^{-1} (horizontal dashed line).

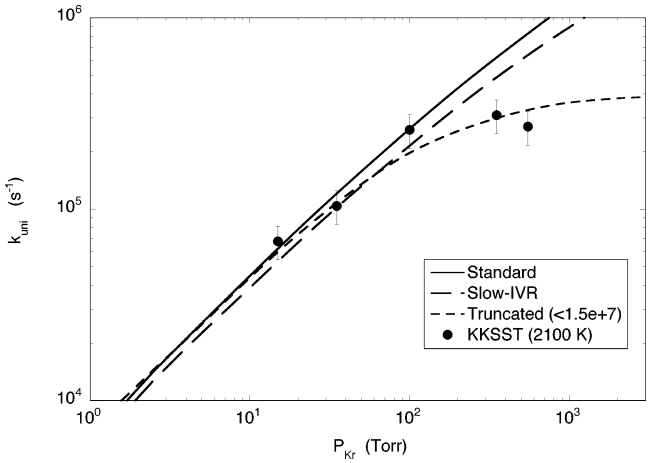

Figure 5. Simulations and experimental data estimated from KKSST: "Standard" is RRKM theory, "slow-IVR" assumes the LRMT IVR theory, and "truncated" assumes the standard RRKM model, but with an upper limit to the microcanonical $k(E) \leq 1.5 \times 10^7$ s^{-1}. All three models use the same energy transfer parameters (see text for details).

well-approximated by a quadratic function of the energy, which facilitates extrapolation of the IVR rate to higher energy

$$k^q_{IVR}(E - E_0)/s^{-1} = 1.1 \times 10^{14} + 1.0 \times 10^{10}(E - E_0) + 2.4 \times 10^5(E - E_0)^2 \quad (13)$$

where E, the vibrational energy, and E_0, the reaction critical energy (24 299 cm^{-1}), are expressed in reciprocal centimeter units. According to this function, $k^q_{IVR}(E_0) \approx 10^{14}$ s^{-1} at the reaction threshold and is increasing rapidly with energy. As noted above, however, energy flow cannot be arbitrarily fast, but is limited to roughly half a vibrational period. Thus, an upper limit of $2\langle\nu\rangle$ is placed on $k^q_{IVR}(E)$ in the calculations, where $\langle\nu\rangle = 3.2 \times 10^{13}$ s^{-1} (corresponding to 1079 cm^{-1}) is the average vibrational frequency in TFE.

The results of three sets of simulations are shown in Figure 5. The data points shown in the figure are from interpolations and short extrapolations of the KKSST data to 2100 K (see Figure 1). For the present purposes, we have assumed that all of the relative errors are ±20%, although the systematic error in the 15 Torr data set is probably larger. The curve labeled

"standard" is the standard RRKM−master equation simulation with fast IVR (described above). The discrepancies between the standard simulation and the KKSST data illustrate the failure of conventional RRKM theory to describe the data at the two highest pressures. The curve labeled "slow-IVR" incorporates the LRMT but assumes that collision-induced IVR is negligible ($k^c_{IVR} = 0$). Since the slow-IVR simulations do not show the sharp rollover toward a high-pressure limit seen in the KKSST data, we conclude that the KKSST data are not consistent with the LRMT-modified RRKM rate.

We note that by neglecting collision-induced IVR, the slow-IVR simulation represents the *maximum* deviation from RRKM theory that is possible according to the LRMT. For the case of *trans*-stilbene isomerization in CH_4 collider gas, LRMT predicts that the collision-induced IVR rate constant is on the order of the total collision rate constant estimated by the Durant−Kaufmann method. If we set k^c_{IVR} for TFE equal to the total rate constant for TFE−Kr collisions (7.6×10^{-9} cm^3 s^{-1}), IVR is very rapid, and the resulting simulation is indistinguishable from the standard model. On the basis of the *trans*-stilbene work and previous studies, we feel that this model, which neglects collision-induced IVR, is unphysical.

Also shown in Figure 5 is a simulation labeled "truncated". This simulation uses standard RRKM theory, but with the additional *arbitrary* assumption that the microcanonical unimolecular rate constant $k(E)$ cannot exceed 1.5×10^7 s^{-1} in the MultiWell simulations. The only justification for this arbitrary assumption is that the resulting simulations are in reasonable agreement with the KKSST pressure-dependent data. It implies that IVR requires a very long period of time (∼67 ns) even at high energies and despite collision-induced IVR. This model has no physical basis, and we feel that it is not realistic, although it fits the KKSST data.

It should be mentioned that all of the simulations at 2100 K (i.e., for the conditions of the KKSST experiments) predict possibly measurable amounts of C−C bond fission according to reaction (−1). For example, at 550 Torr the standard and truncated models predict ∼0.1% and ∼1% yields of free radicals, respectively. Free radical reactions were neglected by KKSST, and we do not know whether these free radical yields can affect the interpretation of the laser schlieren experiments.

Chemical Activation. We also simulated the chemical activation experiments of Marcoux and Setser,[19] in which excited TFE was produced at 300 K with ∼101 kcal mol^{-1} of vibrational excitation.[24,28] In our master equation simulations, we employed the chemical activation distribution function at 300 K for the initial energy distribution and calculated the fraction of TFE stabilized in collisions with krypton collider gas.

For comparisons between the KKSST shock tube data at 2100 K and the Marcoux and Setser chemical activation data at 300 K, it is convenient to assume an energy-independent value of α. For a single-channel unimolecular reaction, it is well-known[4] that a simple energy-independent α produces excellent results, corresponding approximately to the value of $\alpha(E_0, T)$ at the reaction critical energy.

Standard and truncated simulations using the energy-independent exponential-down model give good agreement with the KKSST experimental results at 100 Torr when α(2100 K) = 1275 ± 100 cm^{-1} (independent of energy). Slow-IVR simulations for the same conditions give α(2100 K) = 1700 ± 100 cm^{-1} (independent of energy). These values may be compared with the values shown in Figure 6 for corresponding simulations of the Marcoux and Setser chemical activation results: 350 cm^{-1} and 225 cm^{-1} (estimated uncertainties of ±10%). The present result for the standard model agrees with the result (350 ± 70 cm^{-1}) found by Marcoux and Setser, who used essentially the same method, although they assumed slightly different transition-state and Lennard-Jones parameters. (The present choice of Lennard-Jones parameters produces a collision rate constant at 300 K that is about 8% larger than that used by Marcoux and Setser.)

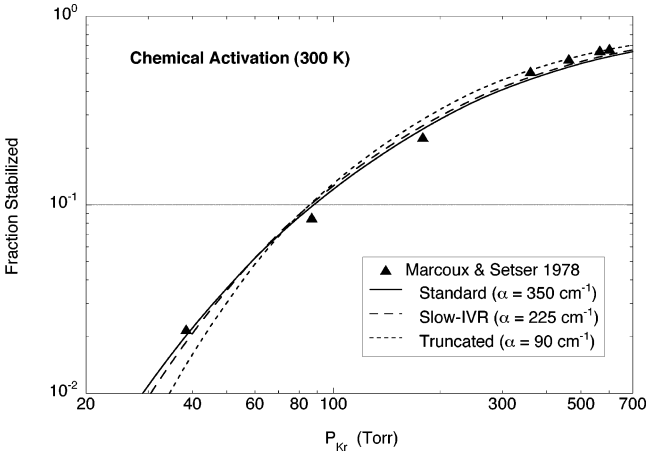

Figure 6. Chemical activation data (300 K) of Marcoux and Setser[19] with simulations according to three models with energy transfer parameter α assumed to be independent of energy.

Although the standard and slow-IVR simulations tend to fit the data slightly better, all three of the chemical activation simulations are in good agreement with the experimental data. In each case, the analysis of the Marcoux and Setser data set relies on the specific assumptions about the unimolecular reaction. Unless a constraint on the energy transfer parameters can be found, the chemical activation experiments do not provide an independent test for the possible effects of slow IVR.

1,1,2-Trifluoroethane. To the best of our knowledge, all of the extant energy transfer data on highly excited 1,1,1-TFE were obtained by analyzing chemical and thermal activation data and hence are dependent on implicit assumptions about the influence of IVR. In the absence of independent data on 1,1,1-TFE, we turn to the 1,1,2-TFE isomer, which may be useful as a proxy.

Energy transfer between argon and the 1,1,2-TFE isomer has been investigated by using a physical "direct" method that does not depend on any assumptions about unimolecular reaction rate constants.[61−63] Infrared multiphoton excitation of the C−F stretching modes was used to prepare highly vibrationally excited populations, which subsequently underwent energy transfer in an argon bath. The vibrational energy transfer was monitored by measuring the intensity of spontaneous infrared fluorescence (IRF) from the C−H stretching modes in the excited molecules. The experiments were analyzed with a full collisional master equation approach (similar to MultiWell) to determine $\alpha(T, E)$ for energy transfer between 1,1,2-TFE and argon. It was found that $\alpha(T, E)$ is essentially independent of temperature from ∼400 K to ∼1000 K and is given by $\alpha_{112}(T, E) = (200 \pm 20) + (0.005 \pm 0.002) \times E$, where E and $\alpha(T, E)$ are expressed in units of reciprocal centimeters.[63]

1,1,2-TFE is an attractive proxy, because it is a geometrical isomer, and hence, most of its vibrational frequencies are similar to those in 1,1,1-TFE. However, it differs from the 1,1,1-TFE isomer in that the torsional mode, which is a symmetric rotor in 1,1,1-TFE, is asymmetric in 1,1,2-TFE. Perhaps more important, the torsion is the lowest vibrational frequency in both molecules, but the frequencies differ: 249 cm^{-1} in 1,1,1-TFE[1,24] and ∼117 cm^{-1} in 1,1,2-TFE.[64,65] Since the lowest vibrational

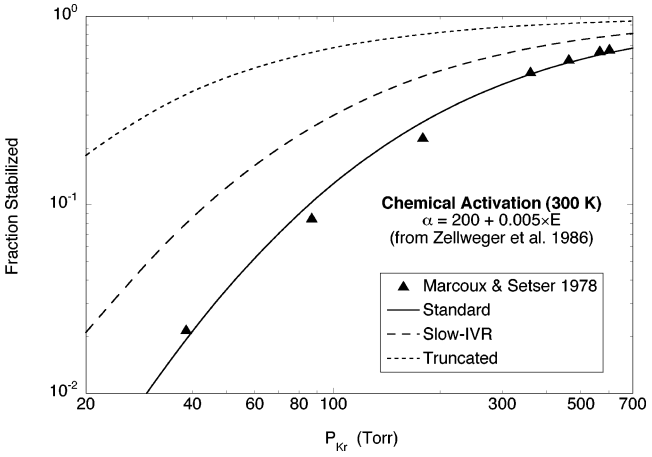

Figure 7. Simulations of the Marcoux and Setser[19] chemical activation data with three rate constant models and assuming $\alpha_{111}(E, T) = \alpha_{112}(E, T)$. The latter quantity was obtained in measurements[63] of Ar + 1,1,2-TFE energy transfer. See text for details.

frequency is often a dominant factor in determining the state-to-state energy transfer rate constant,[31,33] we expect that $\alpha_{112}(T, E)$ for 1,1,2-TFE is unlikely to be smaller than $\alpha_{111}(T, E)$ for 1,1,1-TFE. Since both torsional frequencies are on the order of kT at 300 K, $\alpha(T, E)$ may be about the same for both molecules under the conditions of the chemical activation experiments.

Argon and krypton are similar in their collisional energy transfer properties.[66] Marcoux and Setser[19] found the same value of $\alpha(T, E)$ for both collider gases in collisions with 1,1,1-TFE. Although the masses and assumed Lennard-Jones parameters for the various collider pairs vary somewhat, the collision rate constants are all very similar. The collision rate constants calculated for Kr + 1,1,1-TFE from the slightly different Lennard-Jones parameters in Marcoux and Setser and in the present work are 3.14×10^{-10} and 3.39×10^{-10} cm^3 s^{-1}, respectively. A similar comparison for rate constants for Ar + TFE from Zellweger et al.[63] and from the present work gives 3.84×10^{-10} and 3.53×10^{-10} cm^3 s^{-1}, respectively. Thus, the parameters for krypton and argon differ by only 10−20%.

In light of this discussion, it seems justified to use the Ar + 1,1,2-TFE energy transfer system as a proxy for the Kr + 1,1,1-TFE system, but with the expectation that $\alpha_{111}(T, E)$ may turn out to be smaller than $\alpha_{112}(T, E)$. Thus, we assumed that $\alpha_{111}(T, E) = \alpha_{112}(T, E)$ in simulations of the Marcoux and Setser chemical activation experiments on the Kr + 1,1,1-TFE system. The results for the standard, slow-IVR, and truncated rate constant models are presented in Figure 7, where the agreement between the standard model and the data is (fortuitously) almost exact.

V. Summary and Concluding Remarks

In agreement with KKSST, we have shown that their unimolecular reaction rate data do not agree well with RRKM theory (standard model). Although the experimental detection of dual relaxation times is suggestive that slow IVR is the explanation for the discrepancy between their data set and RRKM theory, we have shown that the dual relaxation most likely originates from energy transfer at energies far below the reaction threshold. In agreement with Kiefer et al.,[30] we conclude that observation of dual relaxation behavior does not necessarily have much to do with the unimolecular reaction.

By implementing the LRMT in the MultiWell master equation code ("slow-IVR" model), we have shown that this IVR theory does not reproduce the sharp leveling-off of the falloff exhibited by the KKSST data set, even when collision-induced IVR is neglected. The neglect of collision-induced IVR is probably unphysical, since it appears to be a necessary feature in successfully describing other systems.[10,67] When collision-induced IVR is included in simulating TFE, the result is indistinguishable from the standard RRKM model, which does not describe the KKSST data very well.

It is, however, possible to simulate the KKSST data if it is arbitrarily assumed that $k(E)$ cannot exceed 1.5×10^7 s^{-1} in the MultiWell simulations (truncated model). The sharp break in the KKSST falloff is reproduced fairly accurately, which is our only justification for truncating $k(E)$ in this way.

Previous shock tube experiments were carried out at lower temperatures and over a range of pressures near the high-pressure limit. Thus, they are not helpful in assessing the KKSST falloff data, although they provide strong support for the transition-state model calculated by KKSST. We have shown that the chemical activation experiments on excited TFE can be successfully fitted with all three of our models, as long as no constraints are placed on assumptions about collisional deactivation of excited TFE. Thus, the existing data on TFE are insufficient to establish whether the KKSST data set is an anomaly.

In an attempt to reach a conclusion, we have used a proxy method to place at least some constraints on the energy transfer parameters in the chemical activation experiments. For this purpose, we have used the geometrical isomer, 1,1,2-TFE, in collisions with argon as a proxy for 1,1,1-TFE in collisions with krypton. Essentially the same agreement between the standard model and the chemical activation data is fortuitous, considering the approximations associated with the use of the proxy and the uncertainties in the measured $\alpha_{112}(T, E)$. However, it is clear that agreement with the other two models is poor. In both cases, the simulations show much more stabilized product than was measured. To bring the simulations into agreement with the data, $\alpha_{111}(T, E)$ for 1,1,1-TFE would have to be ∼1/3.3 times as large as $\alpha_{112}(T, E)$ for 1,1,2-TFE for the truncated model. In comparing values of α for pairs of molecules at high energies, we find $\alpha_{toluene}/\alpha_{benzene} \approx 2.2$ at $E = 30\,000$ cm^{-1} from infrared fluorescence "direct" experiments,[68] $\alpha_{C6F6}/\alpha_{C6H6} \approx 2$ at $E = 24\,000$ cm^{-1} from trajectory calculations,[69] and $\alpha_{toluene}/\alpha_{c-heptatriene} \approx 1-2$ at $E = 40\,000$ cm^{-1} from "direct" ultraviolet absorption experiments.[70,71] The ratio $\alpha_{112}(T, E)/\alpha_{111}(T, E) \approx 3.3$ is at the extreme end of the range of this small collection of examples. Because of the scarcity of energy transfer information, it is not possible to ascertain with certainty whether this ratio is realistic for two such geometrical isomers. Despite the uncertainty associated with using a proxy, we conclude that the standard model is significantly more consistent with the Marcoux and Setser chemical activation data set than are the two non-RRKM models.

In the preceding sections, we have examined the KKSST data set closely and confirmed that it is not well described by RRKM theory (standard model). Unfortunately, the present model calculations can neither confirm nor rule out the possibility that this is a non-RRKM reaction: the evidence on both sides is weak. Many reasons can be given why TFE should be well-described by RRKM theory, but arguments can also be made in support of the non-RRKM interpretation. In Appendix III, we outline arguments by Kiefer and KKSST that support TFE as a non-RRKM system. We also provide counter arguments to challenge their interpretation.

Finally, although it is not possible to determine with confidence whether non-RRKM effects are important or whether the KKSST data are in error, the KKSST data set clearly has unexplained systematic errors at the lowest pressure. It is possible that the rate constants at the highest two pressures are also affected by unknown systematic errors. Additional work (computational and experimental) is needed to resolve this issue. Nonetheless, RRKM theory has a long history of success on many systems. Until stronger evidence of a breakdown of the theory is available for this type of reaction, we feel that RRKM theory is still the method of choice.

Acknowledgment. This paper celebrates Jürgen Troe, who has long been an outstanding leader in chemical kinetics and shock tube studies. Thanks go to John H. Kiefer for discussions and for providing the KKSST data set in tabular form. Thanks also go to Bert E. Holmes, Lawrence L. Lohr, and Lawrence Harding for helpful discussions. At Michigan, this work was funded in part by NSF (Atmospheric Chemistry Division), NASA (Upper Atmosphere Research Program), and NASA (Planetary Atmospheres). At Nevada, this work was funded by NSF grant no. CHE-0512145. Keith D. King thanks the University of Adelaide for a short period of study leave during which part of this work was carried out.

Appendix I. Reaction Path Degeneracy

There is some confusion in the literature about the reaction path degeneracy for HF elimination from TFE. In summary, (a) KKSST used 9, (b) in their earlier papers, Setser and co-workers[19,27] and Holmes and co-workers[24] both used 6, and (c) in a recent paper, Ferguson et al.[28] used 9. Explanations given were that the reaction path degeneracy should be 9 if there is free rotation about the C−C bond, but if the rotor is treated as a vibration, then it must be 3.

However, if one follows the arguments outlined in Gilbert and Smith,[4] then there are 9 transition states and 3 equivalent potential wells (due to the threefold internal rotor symmetry). Six transition states are accessed from each potential well via an internal rotation of $\pm 2\pi/6$ and choosing any one of the resulting HF pairings. Half of the initial population in each well goes to each of the transition states. Since $^1/_3$ of the initial population is in each well, the path degeneracy is $(^1/_3) \times (^1/_2) \times (3 \text{ wells}) \times (6 \text{ paths/well}) = 3$ paths. (The only way to arrive at a path degeneracy of 6 is to neglect the threefold internal rotor symmetry so that there is only 1 well with 6 accessible transition states.)

Appendix II. RRKM Model Parameters

Except for minor revisions, the RRKM model for HF elimination from TFE was taken from KKSST. Their model is very similar to the models described by Holmes and co-workers.[24,28] See the text for further discussion of the model.

For the chemical activation reaction of $CF_3 + CH_3 \rightarrow$ TFE, the inverse Laplace transform (ILT) method[2,3,72] was used, which only requires specification of the Arrhenius *A*-factor and activation energy, which can be identified approximately with the critical energy: $A = 1 \times 10^{16}$ s^{-1} and $E_0 = 101.0$ kcal mol^{-1}.

For the sake of completeness, the principal model parameters are summarized in Table A1.

TABLE A1: RRKM Model[a] for $CF_3CH_3 \rightarrow CF_2CH_2 + HF$

vibrational frequencies (cm^{-1}) and degeneracies (molecule): 3330(2), 3246(1), 1627(2), 1600(1), 1429(1), 1414(2), 1094(2), 907(1), 645(1), 584(2), 391(2), 249(1)[b]
vibrational frequencies (cm^{-1}) and degeneracies (transition state): 3428(1), 3332(1), 1875(1), 1710(1), 1617(1), 1552(1), 1452(1), 1128(1), 1023(1), 971(1), 796(1), 656(1), 524(1), 507(1), 428(1), 298(1), 260(1)
moments of inertia (amu·Å^2)
molecular (2D) adiabatic: 331.38
transition state (2D) adiabatic: 389.98
molecular active (1D): 310.53[c]
transition state active (1D): 309.82[c]
reaction path degeneracy: 3
E_o (kcal/mol): 69.45
ΔH_f(0 K) (kcal/mol): 31.8
Kr: $\sigma_{Kr} = 3.61$ Å; $\epsilon_{Kr}/K = 190$
TFE: $\sigma_{TFE} = 3.47$ Å; $\epsilon_{TFE}/K = 114$
molecular masses (g mol^{-1}): $M_{Kr} = 83.80$; $M_{TFE} = 84.04$

[a] Most model parameters are taken from KKSST. [b] Vibration treated as a hindered rotor ($\sigma = 3$) with a barrier to rotation of 1137 cm^{-1}. [c] External rotor treated as a quantum rotation (qro) within MultiWell.

Appendix III. A Critique of the KKSST Non-RRKM Model

KKSST[1] and Kiefer (private communication) suggest that their data can be explained by a non-RRKM model in which a subset of vibrational modes is preferentially excited by collisions following the shock. This subset of modes sequesters vibrational energy, which flows only very slowly to the reaction coordinate. Thus, when TFE has energy greater than the reaction critical energy, it reacts at a rate controlled by slow ($\sim 10^8$ s^{-1}) IVR between the sequestering modes and the others. KKSST also assume collision-enhanced IVR, and collisional excitation of the modes that are coupled to the reaction coordinate is insignificant. Kiefer envisions rapid collisional energy transfer mostly to the torsion, which remains only weakly coupled to the other modes at high energies due to high symmetry. Furthermore, when the torsion is excited, the distortion of CH_3 and CF_3 rotors needed to achieve the geometry of the transition state introduces a >20 kcal mol^{-1} increase in the energy requirement for reaction. This conclusion is based on a calculation carried out by L. Harding in which the two distorted rotors were "frozen" in the transition state geometry and forced to rotate around the C−C axis (L. Harding and J. H. Kiefer, private communication). This added energy effectively raises the critical energy for reaction when the torsion is excited, resulting in the non-RRKM effect. Thus, excitation of the isolated torsion both sequesters energy, making it unavailable for reaction, and increases the reaction critical energy, further slowing the reaction. KKSST also suggest that chemically activated TFE formed by recombination of $CF_3 + CH_3$ results in little excitation of the torsion. Thus, the chemical activation experiments result in RRKM behavior, while collisional activation, which preferentially excites the torsion, results in non-RRKM behavior.[1]

There are a number of points in this qualitative model where, in our opinion, one can reach different conclusions. The torsion barrier in TFE is ~ 1137 cm^{-1}, and the harmonic frequency is ~ 249 cm^{-1}. Below this torsion barrier, the torsional states are nearly equally spaced (like harmonic oscillator states), and collisional activation from one torsion state to the next will proceed with roughly the same rate constant, scaled by the vibrational quantum number.[33] Above the barrier, however, the torsion states become more like free internal rotations where the state energy gaps become larger at higher energies. At a torsional energy of ~ 20 kcal mol^{-1}, for example, the hindered rotor states in TFE are about 400 cm^{-1} apart. As the energy gaps increase, collisional excitation from one state to the next will become slower, because of the Boltzmann factor. Thus,

there is an internal limitation in the rate of ladder climbing up the pure torsional levels. Conventional wisdom would then predict that, when the energy gaps become large enough, further ladder climbing would take place not by pure torsional excitations, but via excitation of combinations of modes, where the energy gaps are smaller (of course, there is a penalty for simultaneous changes of more than one quantum number[32,33,73]). However, we do not know how much energy would have to be sequestered to account for the proposed non-RRKM effects.

But are the torsions isolated from other modes? At low energy, none of the modes are expected to strongly couple to other modes. The LRMT predicts an IVR threshold near 3500 cm^{-1} and rapid IVR at high internal energy. Classical trajectory calculations on ethane[74] indicate that the torsion acts largely like a free rotor at moderate energies above the torsion barrier. Because it is coupled *both* to the overall molecular rotations *and* to the molecular vibrations, the torsion acts as an efficient "gateway" to collisional energy transfer, which is mediated by rotations.[74] Thus, the torsion in ethane is not isolated, despite its high symmetry. We surmise that this is because excitation of the CH_3 deformation and asymmetric stretch modes lowers the symmetry of the rotors and causes resistance to rotation; this introduces coupling between the torsion and the other modes. The same process should be operative in TFE.

We also challenge Kiefer and Harding's assertion that placing energy in the torsion inhibits the reaction by introducing an additional potential energy barrier. We argue that the effect of distorting the spinning rotors in this way is instead more likely to provide a mechanism for *faster* IVR between the torsion and the other modes (mostly the bending modes and CX_3 deformations), resulting in randomization of energy. We surmise that distortions in the rotors that introduce resistance to the rotation will result in transfer of energy between the two types of internal modes.

Is collision-induced IVR negligible for this system? It is safe to say that IVR is not completely understood and continues to be a topic of active investigation. The scant evidence available, however, indicates that collision-induced IVR is important. In the isomerization of photoexcited stilbene in high pressures of CH_4, collision-induced IVR must be included[10] with a rate constant (8.3×10^{-9} cm^3 s^{-1}) which is close to the total collision rate constant (12.9×10^{-9} cm^3 s^{-1}) estimated using the approximate method of Durant and Kaufman.[75] Note that the total collision rate constant is much larger than the Lennard-Jones collision rate constant. The importance of collision-induced IVR is also supported by trajectory calculations.[48,67] The LRMT is reasonably successful in modeling[76] stilbene isomerization in a number of bath gases at pressures up to 10 bar or more[77] when collision-induced IVR is included. These calculations show that monatomic colliders are less efficient than polyatomic ones, but the rate constants are still very large.[76] Thus, we conclude that collision-induced IVR in TFE is likely to be very important at the higher pressures in the KKSST experiments.

Thus, there are considerable uncertainties surrounding the KKSST qualitative non-RRKM model. Many of the arguments on both sides are speculative. We note that many of these arguments can be tested using classical trajectory calculations. Such calculations are underway in this laboratory, and the results will be reported in a future publication.[20] Preliminary results indicate that, for energies below the reaction threshold, energy in the torsional mode does not remain isolated from the other vibrational degrees of freedom.

References and Notes

(1) Kiefer, J. H.; Katapodis, C.; Santhanam, S.; Srinivasan, N. K.; Tranter, R. S. *J. Phys. Chem. A* **2004**, *108*, 2443.
(2) Forst, W. *Theory of Unimolecular Reactions*; Academic Press: New York, 1973.
(3) Forst, W. *Unimolecular Reactions. A Concise Introduction*; Cambridge University Press: Cambridge, 2003.
(4) Gilbert, R. G.; Smith, S. C. *Theory of Unimolecular and Recombination Reactions*; Blackwell Scientific: Oxford, 1990.
(5) Holbrook, K. A.; Pilling, M. J.; Robertson, S. H. *Unimolecular Reactions*, 2nd ed.; Wiley: Chichester, 1996.
(6) Robinson, P. J.; Holbrook, K. A. *Unimolecular Reactions*; Wiley-Interscience: New York, 1972.
(7) Leitner, D. M. *Adv. Chem. Phys.* **2005**, *130* (Part B), 205.
(8) Leitner, D. M.; Wolynes, P. G. *Phys. Rev. Lett.* **1996**, *76*, 216.
(9) Leitner, D. M.; Wolynes, P. G. *Chem. Phys. Lett.* **1997**, *280*, 411.
(10) Leitner, D. M.; Levine, B.; Quenneville, J.; Martinez, T. J.; Wolynes, P. G. *J. Phys. Chem. A* **2003**, *107*, 10706.
(11) Gruebele, M.; Wolynes, P. G. *Acc. Chem. Res.* **2004**, *37*, 261.
(12) Barker, J. R. *Int. J. Chem. Kinet.* **2001**, *33*, 232.
(13) Barker, J. R.; Ortiz, N. F.; Preses, J. M.; Lohr, L. L. MultiWell-1.4.1 software; Ann Arbor, Michigan, 2004; http://aoss.engin.umich.edu/multiwell/.
(14) Tschiukow-Roux, E.; Quiring, W. J. *J. Phys. Chem.* **1971**, *75*, 295.
(15) Cadman, P.; Day, M.; Trotman-Dickenson, A. F. *J. Chem. Soc. A* **1971**, 1356.
(16) Tsang, W.; Lifshitz, A. *Int. J. Chem. Kinet.* **1998**, *30*, 621.
(17) Mitin, P. V.; Barabanov, V. G.; Volkov, G. V. *Kinet. Catal.* **1988**, *29*, 1279.
(18) Marcoux, P. J.; Siefert, E. E.; Setser, D. W. *Int. J. Chem. Kinet.* **1975**, *7*, 473.
(19) Marcoux, P. J.; Setser, D. W. *J. Phys. Chem.* **1978**, *82*, 97.
(20) Stimac, P. J.; Barker, J. R. To be published.
(21) Sianesi, D.; Nelli, G.; Fontanelli, R. *Chim. Ind. (Milan)* **1968**, *50*, 619.
(22) Tsang, W. *Int. J. Chem. Kinet.* **1973**, *5*, 643.
(23) Rodgers, A. S.; Ford, W. G. F. *Int. J. Chem. Kinet.* **1973**, *5*, 965.
(24) Martell, J. M.; Beaton, P. T.; Holmes, B. E. *J. Phys. Chem. A* **2002**, *106*, 8471.
(25) Pettijohn, R. R.; Mutch, G. W.; Root, J. W. **1975**, *79*, 2077.
(26) Neely, B. D.; Carmichael, H. **1972**, *76*, 954.
(27) Chang, H. W.; Craig, N. L.; Setser, D. W. *J. Phys. Chem.* **1972**, *76*, 954.
(28) Ferguson, J. D.; Johnson, N. L.; Kekenes-Huskey, P. M.; Everett, W. C.; Heard, G. L.; Setser, D. W.; Holmes, B. E. *J. Phys. Chem. A* **2005**, *109*, 4540.
(29) Kiefer, J. H.; Buzyna, L. L.; Dib, A.; Sundaram, S. *J. Chem. Phys.* **2000**, *113*, 48.
(30) Kiefer, J. H.; Santhanam, S.; Srinivasan, N. K.; Tranter, R. S.; Klippenstein, S. J.; Oehlschlaeger, M. A. *Proc. Combust. Inst.* **2004**, *30*.
(31) Lambert, J. D. *Vibrational and Rotational Relaxation in Gases*; Clarendon Press: Oxford, 1977.
(32) Lambert, J. D.; Salter, R. *Proc. R. Soc. London, Ser. A* **1959**, *253*, 277.
(33) Yardley, J. T. *Introduction to Molecular Energy Transfer*; Academic Press: New York, 1980.
(34) Holmes, R.; Jones, G. R.; Pusat, N. *J. Chem. Phys.* **1964**, *41*, 2512.
(35) Herzfeld, K. F.; Litovitz, T. A. *Absorption and Dispersion of Ultrasonic Waves*; Academic Press: New York, 1959.
(36) Schwartz, R. N.; Slawsky, Z. I.; Herzfeld, K. F. *J. Chem. Phys.* **1952**, *20*, 1591.
(37) Clary, D. C. *J. Phys. Chem.* **1987**, *91*, 1718.
(38) Clary, D. C.; Kroes, G. J. Coupled quantum scattering calculations. In *Vibrational Energy Transfer Involving Large and Small Molecules*; Barker, J. R., Ed.; JAI Press Inc.: Greenwich, CT, 1995; Vol. 2A, p 135.
(39) Curtiss, L. A.; Raghavachari, K.; Redfern, P. C.; Rassolov, V.; Pople, J. A. *J. Chem. Phys.* **1998**, *109*, 7764.
(40) Barker, J. R.; Ortiz, N. F.; Preses, J. M.; Lohr, L. L. MultiWell-1.5.1g software (development version), Ann Arbor, Michigan, 2005.
(41) Barker, J. R.; Shovlin, C. N. *Chem. Phys. Lett.* **2004**, *383*, 203.
(42) Beyer, T.; Swinehart, D. F. *Comm. Assoc. Comput. Machines* **1973**, *16*, 379.
(43) Stein, S. E.; Rabinovitch, B. S. *J. Chem. Phys.* **1973**, *58*, 2438.
(44) Shi, J.; Barker, J. R. *Int. J. Chem. Kinet.* **1990**, *22*, 187.
(45) Barker, J. R.; King, K. D. *J. Chem. Phys.* **1995**, *103*, 4953.
(46) Barker, J. R.; Yoder, L. M.; King, K. D. *J. Phys. Chem. A* **2001**, *105*, 796.
(47) Leitner, D. M. *Int. J. Quantum Chem.* **1999**, *75*, 523.
(48) Nordholm, S.; Back, A. *Phys. Chem. Chem. Phys.* **2001**, *3*, 2289.
(49) Nordolm, S. *Chem. Phys.* **1989**, *137*, 109.
(50) Keske, J. C.; Pate, B. H. *Annu. Rev. Phys. Chem.* **2000**, *51*, 323.
(51) Baer, T.; Potts, A. R. *J. Phys. Chem. A* **2000**, *104*, 9397.

(52) Chandler, D.; Kuharski, R. A. *Faraday Discuss. Chem. Soc*. **1988**, *85*, 329.
(53) Leitner, D. M.; Wolynes, P. G. *J. Chem. Phys.* **1996**, *105*, 11226.
(54) Logan, D. E.; Wolynes, P. G. *J. Chem. Phys.* **1990**, *93*, 4994.
(55) Bigwood, R.; Gruebele, M. *Chem. Phys. Lett.* **1995**, *235*, 604.
(56) Bigwood, R.; Gruebele, M.; Leitner, D. M.; Wolynes, P. G. *Proc. Natl. Acad. Sci. U.S.A.* **1998**, *95*, 5960.
(57) Pearman, R.; Gruebele, M. *J. Chem. Phys.* **1998**, *108*, 6561.
(58) Madsen, D.; Pearman, R.; Gruebele, M. *J. Chem. Phys.* **1997**, *106*, 5874.
(59) Kiefer, J. H. The Laser-schlieren Technique. In *Shock Waves in Chemistry*; Lifshitz, A., Ed.; Marcel Dekker: New York, 1981; p 219.
(60) Davis, M. J.; Kiefer, J. H. *J. Chem. Phys.* **2002**, *116*, 7814.
(61) Zellweger, J. M.; Brown, T. C.; Barker, J. R. *J. Chem. Phys.* **1985**, *83*, 6251.
(62) Zellweger, J. M.; Brown, T. C.; Barker, J. R. *J. Chem. Phys.* **1985**, *83*, 6261.
(63) Zellweger, J. M.; Brown, T. C.; Barker, J. R. *J. Phys. Chem.* **1986**, *90*, 461.
(64) Kalasinsky, V. F.; Anjaria, H. V.; Little, T. S. *J. Phys. Chem.* **1982**, *86*, 1351.
(65) Chen, Y.; Paddison, S. J.; Tschuikow-Roux, E. *J. Phys. Chem.* **1994**, *98*, 1100.
(66) Tardy, D. C.; Rabinovitch, B. S. *Chem. Rev.* **1977**, *77*, 369.
(67) Bolton, K.; Nordholm, S. *Chem. Phys.* **1996**, *206*, 103.
(68) Barker, J. R.; Brenner, J. D.; Toselli, B. M. The Vibrational Deactivation of Large Molecules by Collisions and by Spontaneous Infrared Emission. In *Vibrational Energy Transfer Involving Large and Small Molecules*; Barker, J. R., Ed.; JAI Press Inc.: Greenwich, CT, 1995; Vol. 2B.
(69) Lenzer, T.; Luther, K.; Troe, J.; Gilbert, R. G.; Lim, K. F. *J. Chem. Phys.* **1995**, *103*, 626.
(70) Hippler, H.; Troe, J.; Wendelken, H. J. *J. Chem. Phys.* **1983**, *78*, 6709.
(71) Heymann, M.; Hippler, H.; Troe, J. *J. Chem. Phys.* **1984**, *80*, 1853.
(72) Forst, W. *J. Phys. Chem.* **1972**, *76*, 342.
(73) Tanczos, F. I. *J. Chem. Phys.* **1959**, *30*, 1119.
(74) Linhananta, A.; Lim, K. F. *Phys. Chem. Chem. Phys.* **1999**, *1*, 3467.
(75) Durant, J. L.; Kaufamn, F. *Chem. Phys. Lett.* **1987**, *142*, 246.
(76) Weston, R. E., Jr.; Barker, J. R. In preparation.
(77) Meyer, A.; Schroeder, J.; Troe, J. *J. Phys. Chem. A* **1999**, *103*, 10528.